Journal of Electroceramics 6:2, 135–146, 2001

The Influence of Bi_2O_3 and Sb_2O_3 on the Electrical Properties of ZnO-Based Varistors

J. OTT,[1,*] A. LORENZ,[1,*] M. HARRER,[1,*] E.A. PREISSNER,[1,*] C. HESSE,[2,†] A. FELTZ,[2,†] A.H. WHITEHEAD[1,*] & M. SCHREIBER[1,*]

[1]*Funktionswerkstoffe F & E GmbH, Marktstrasse 3, A-7000 Eisenstadt, Austria*

[2]*EPCOS OHG, Seimensstrasse 43, A-8530 Deutschlandsberg, Austria*

Submitted July 12, 2000; Revised December 7, 2000; Accepted December 15, 2000

Abstract. This work presents a study of the influence of both Bi content and Sb/Bi ratio on the electrical characteristics of a commercial-type ZnO varistor. In contrast to previous studies two nonlinear coefficients, the breakdown fields and energy absorption abilities were measured after sintering at 970°C or 930°C. The Bi-content was varied from 0.9 to 1.8 at% while the Sb/Bi ratio was varied from 0.8 to 1.5, leading to values of up to 104 for the nonlinear coefficient $\alpha 1$, 1100 V mm^{-1} for the breakdown field and 1137 J cm^{-3} for the energy absorption ability. The highest α value was measured for the highest Bi-content and the lowest Sb/Bi ratio and vice versa. The breakdown field E_V increased with lower sintering temperature, increased Sb/Bi ratio (at a given Bi-content) and increased Bi-content (at a given Sb/Bi ratio). The energy absorption coefficient increased at the higher sinter temperature and with lower Sb and Bi concentrations.

The observed effects were related to the amount of spinel phase ($Zn_7Sb_2O_{12}$) formed during the sintering process and the amount of liquid phase present during early stages of the sintering process.

Keywords: ZnO-based varistors, bismuth oxide, antimony oxide, energy absorption, nonlinearity coefficient

Introduction

ZnO varistors are polycrystalline ceramics containing various minor components. They exhibit extremely nonlinear voltage/current (*V/I*) characteristics, as shown for a typical device in Fig. 1 [1]. The nonlinear region of some ZnO materials extends over several orders of magnitude in current. This extensive non-Ohmic behaviour together with an ability to repeatedly withstand relatively high power pulses has resulted in their widespread application as voltage surge protectors in electrical circuits. The primary function of commercial varistors is to protect electrical equipment by rapidly discharging transient current surges and hence limiting the potential difference across the device. As can be seen from a typical *V/I* curve, transient surges with current densities in the upturn region (Fig. 1) are accompanied by rather high voltages per unit thickness. This corresponds to rather high energies per unit volume that must be tolerated by the varistors. Hence, typical maximum energy absorption capabilities W, expressed in J cm^{-3}, are occasionally specified for varistors. The W value of a given varistor is also dependent on wave shape of the pulse [2]. For this study we have chosen the wave shape of a lightning surge, an 8×20 μs pulse.

It is known that the device nonlinearity is dependent on the density and chemical composition of the grain boundaries: bodies containing large grains, and hence few grain boundaries, or with very low impurity levels tend to exhibit more linear I-V curves. The behaviour of the intergranular regions is often modelled as a double Schottky barrier (DSB), with the additives represented as bulk or interfacial defect states. However, the exact role of the minor components is often

*Formerly with Austrian Research Centre Seibersdorf, A-2444 Seibersdorf, Austria.

†Formerly with Seimens-Matsushita, A-8530 Deutschlandsberg, Austria.

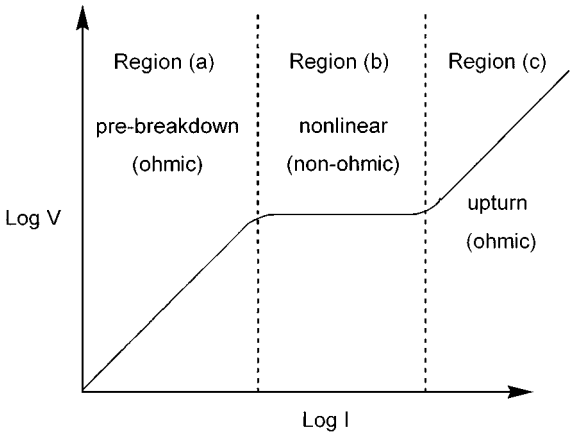

Fig. 1. Logarithmic *I/V* curve of a ZnO varistor, divided into three characteristic regions.

hard to assess, with commercially available ZnO varistors consisting of up to 10 different oxides (such as Bi_2O_3, Sb_2O_3, CoO, MnO, Cr_2O_3, SiO_2, NiO) [3–7]. Depending on the amount, location and function, they are sometimes distinguished as dopants and additives. Dopants are typically those that enhance the conductivity within the ZnO grain. Additives are mostly responsible for the liquid phase sintering process, during which the Schottky barriers are formed. Despite a large amount of research on the effect of the different oxides on the electrical properties, the influence of the amount of additive oxides and especially their mutual interdependences are still not well understood.

Of special interest are the common additives Bi_2O_3 and Sb_2O_3. The ZnO-Bi_2O_3 system has a eutectic at 750°C [8], which gives rise to liquid formation and hence to grain growth during sintering. Bi_2O_3 is crucial for the barrier formation by forming very thin amorphous Bi rich films (1–2 nm) or intergranular segregation of Bi_2O_3 at ZnO/ZnO grain boundaries [9–11]. The remaining Bi_2O_3 phases are suspected to contribute to leakage current and degradation mechanisms after cooling [12]. Previous studies have shown that increasing the Bi content between 1.1 and 4.6 at% in the absence of Sb, after sintering at 1000°C, caused the average grain size to increase [13] contradicting previous findings that between 1.0 and 4.0 at% Bi the grain size decreased [14] and that grain size remained roughly constant above 0.3 at% Bi [15].

With the addition of Sb the system is further complicated as Sb_2O_3, Bi_2O_3 and ZnO can form a pyrochlore phase ($Zn_2Sb_3Bi_3O_{14}$) at low temperatures which decomposes to a spinel phase ($Zn_7Sb_2O_{12}$) above 900°C by reaction with ZnO [16]. By varying the Bi content from 2.0–5.1 at% at a constant Sb /Bi ratio of 2 the nonlinear coefficient was found to have higher values at 2.0 and 4.3 at% ($\alpha \sim 30$) than 3.4 or 5.1 at% ($\alpha \sim 18$) [17]. It was also reported that varying the Sb/Bi ratio between 0.3 to 17 (at a constant 3.0 at% Bi) resulted in a maximum in the nonlinearity coefficient ($\alpha = 55$) at a ratio of ∼2.3 after sintering at 1200°C [18]. Ito et al. [19] found that increasing the Sb/Bi ratio from 0.002 to 0.2 (at a constant 1.0 at% Bi) caused retardation of grain growth during sintering at 1000°C.

The growth of ZnO grains has been found to be inhibited by spinel grains, which must obtain a certain minimum size in order to be effective pinning points for the migration of grain boundaries. The pyrochlore phase has also been found to inhibit grain growth [20].

In order to obtain a high performance varistor with high breakdown voltages and high energy absorption capabilities it was considered necessary to develop varistor ceramics with small and homogeneously distributed grain sizes. To meet these demands it is necessary to develop powders which start to compact at low sintering temperatures and which are able to form sufficient spinel to inhibit grain growth and widening of the grain size distribution. On the first sight these demands could be met by the use of suitable amounts of Bi_2O_3 and a high Sb/Bi ratio. However, large amounts of intergranular phases originating from Bi_2O_3 and Sb_2O_3 phases may increase the leakage currents and decrease the maximum discharging capabilities and should therefore be avoided.

In this paper we studied the influence of variations of the Bi_2O_3 content (0.9–1.8 at% Bi) versus the Sb/Bi ratio (0.8–1.5) on the electrical characteristics and energy absorption capability at low sintering temperatures. This study differs from previous ones [13, 14, 17–20] in that several electrical characteristics (two nonlinearity coefficients and the breakdown field) together with the energy absorption ability of the varistors were considered and, to avoid complications from unquantified distribution of the Bi and Sb through the grain bulks, a precipitation technique was used to place the additives at the grain boundaries. Previous studies have tended to report a limited number of characteristics which cannot readily be compared due to differing preparative conditions (composition, sintering temperature, and so on).

Experimental Procedure

Varistor Preparation

Starting from a composition based on commercially available varistors the powders were prepared by precipitation of the dopant salts on pure ZnO powder from aqueous solution. A detailed description of the baseline preparation technique is published elsewhere [21].

A single batch of the doped ZnO powder was prepared. This batch was divided into 9 parts and to each of these parts different amounts (Table 1) of additives, responsible for the formation of the liquid phase and inhibition of grain growth during sintering, were added. The average size of the primary particles after addition of minor components was 0.5–0.8 μm (as measured by laser diffraction).

After drying in a rotary evaporator the powders were calcined in ambient atmosphere at 480°C for 4 h. The calcined powders were ground and 2.0% of binder was added. The powders were then uniaxially pressed into pellets with a green body density of approximately 55.0% of the theoretical maximum. The pellets were heated at a rate of 3 K min^{-1} until the maximum temperature of either 930°C (denoted 1a–9a) or 970°C (denoted 1b–9b) was obtained. After maintaining the maximum temperature for 90 min the samples were cooled to room temperature at a rate of 1 K min^{-1}. The resulting dark grey ceramic bodies were of approximately 8 mm diameter and 1.15 mm height. The densities of the sintered bodies (Table 1) were $94.4 \pm 2.1\%$ of the theoretical maxima after sintering at 930°C or $96.6 \pm 1.4\%$ after sintering at 970°C, which compares well with literature values for higher temperature sintering (1100–1300°C) of $92.5 \pm 5.5\%$ [7].

Table 1. Additive compositions and sinter body densities of varistor samples.

Sample	Bi content/ at%	Sb/Bi ratio	Density/% of theoretical a (930°C)	b (970°C)
1	1.8	0.8	93.6	97.2
2	1.8	1.2	92.3	95.2
3	1.8	1.5	93.2	96.8
4	1.3	0.8	95.6	97.2
5	1.3	1.2	96.4	96.4
6	1.3	1.5	94.1	97.5
7	0.9	0.8	96.3	97.5
8	0.9	1.2	95.4	97.9
9	0.9	1.5	94.5	97.0

Scanning electron microscopy was performed on polished pellets after thermal etching (20 min at 800°C) to elucidate the microstructure. The accelerating voltage was 10 KeV.

Electrical Measurements

In order to measure the electrical properties the samples were contacted with silver paste. The *V/I* characteristics were measured at five different currents 1 μA, 10 μA, 100 μA, 1 mA and 10 A. In the range 1 μA to 1 mA d.c. measurements were taken, however at 10 A an 8×20 μs shaped pulse was used to avoid excessive heating of the samples. The 8×20 μs pulse, in which the current rises to a maximum in 8 μs and then decays to 50% of its maximum value after a further 20 μs, is sometimes used to simulate the current surge arising from a lightening strike.

In excess of 30 pellets were measured for each of the nine samples in order to obtain representative *V/I* relationships. To characterise the *V/I* behaviour of different ZnO varistors the breakdown field E_V and two nonlinearity coefficients $\alpha 1$ and $\alpha 2$ were evaluated by the relationships given in Eqs. (1) and (2).

$$E_V = \frac{V_b}{d} \tag{1}$$

$$\alpha = \frac{\log\left(\frac{I_2}{I_1}\right)}{\log\left(\frac{V_2}{V_1}\right)} \tag{2}$$

where V_b is the breakdown voltage, d is the sample thickness, V_1 and V_2 are the voltages measured at the currents I_1 and I_2 respectively. The breakdown voltage marks the transition from the Ohmic pre-breakdown region to the nonlinear region (Fig. 1). Because of the lack of sharpness of the transition in the *V/I* curves it was difficult to determine the exact location of the breakdown voltage. Therefore we chose to define the breakdown voltage (V_b) at a current of 1 mA (approximately equivalent to 2 mA cm^{-2} for our sample geometry), a value that has often been used [22]. Indeed, our previous experience has shown that for most varistors the E_V values thus obtained were close to the onset of nonlinearity when full *I/V* curves were examined.

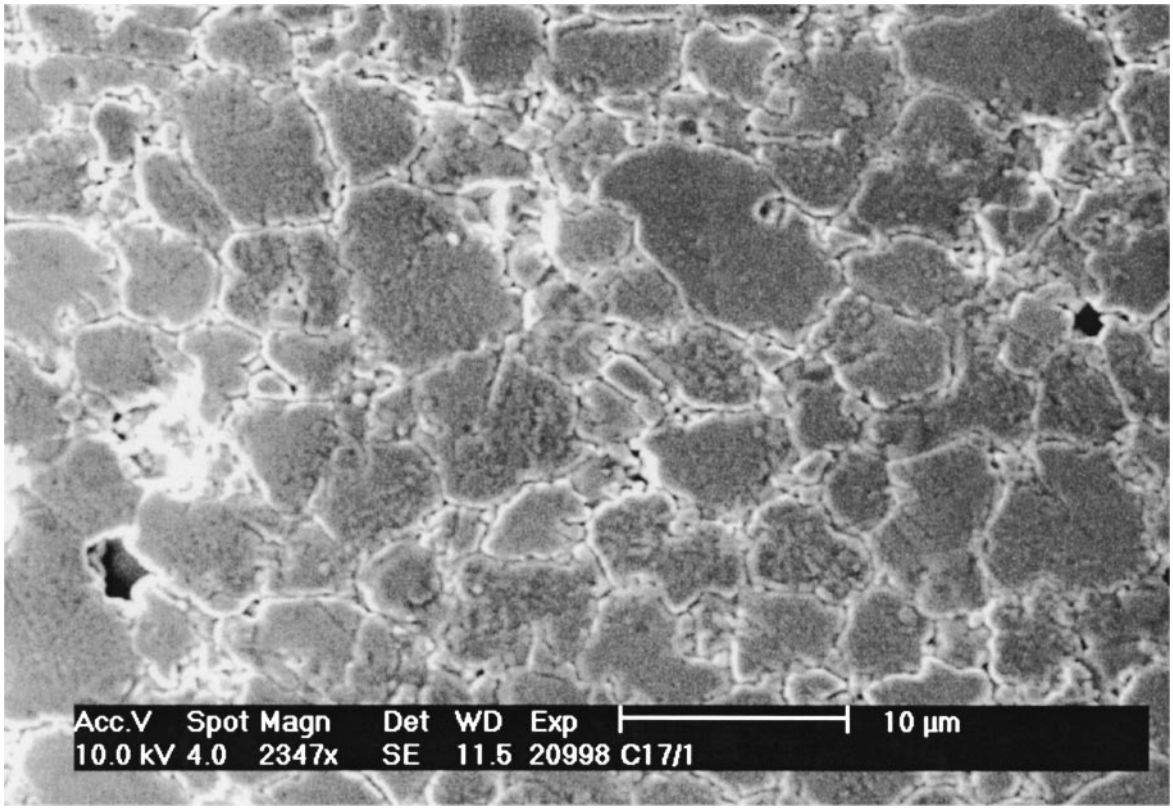

Fig. 2. Typical scanning electron micrograph (secondary electron detector) of a sintered, polished and thermally etched varistor pellet (sample 9a).

$\alpha 1$ was measured when $I_1 = 10\ \mu$A and $I_2 = 1$ mA and $\alpha 2$ when $I_1 = 1$ mA and $I_2 = 10$ A. Typically $\alpha 1$ described the nonlinearity of the *V/I* response in the breakdown (nonlinear) region, possibly extending to the region of transition between pre-breakdown and breakdown responses. $\alpha 2$ gave some indication of the width of the nonlinear region and the degree of protection afforded by the device. A higher value of $\alpha 2$ would tend to indicate a wider nonlinear region and better protection against current surges.

The energy absorption capability of a given composition was examined with five samples. The varistors were treated with pulses of $8 \times 20\ \mu$s wave shape with increasing current. After each pulse the breakdown field at 1 mA (E_V) was measured. It was considered that maximum energy absorption, W, had been exceeded when one of the five varistor pellets was destroyed or the change in E_V was greater than 10%.

Results

All of the compositions led to dense ceramic bodies after sintering at 930°C or 970°C, with microstructures similar to that shown in Fig. 2. In addition each of the sintered bodies exhibited typical nonlinear *V/I* behaviour that enabled evaluation of parameters commonly used to characterise varistors.

From Figs. 3 and 4 it may be noted that E_V tended to increase with increasing Bi content and increasing Sb/Bi ratio. At the lower sintering temperature the E_V value for a sample of given Sb and Bi concentration was significantly higher than at 970°C. The range of E_V values was also greater at the lower sintering temperature (480 V mm^{-1} compared to 240 V mm^{-1}).

Figures 5 and 6 show $\alpha 1$ values arranged against Bi content and Sb/Bi ratio for varistors sintered at 930°C and 970°C respectively. The $\alpha 1$ values obtained were distributed between a value of 46 (sample 9a) which is typical of commercial samples [7, 22, 23], to the

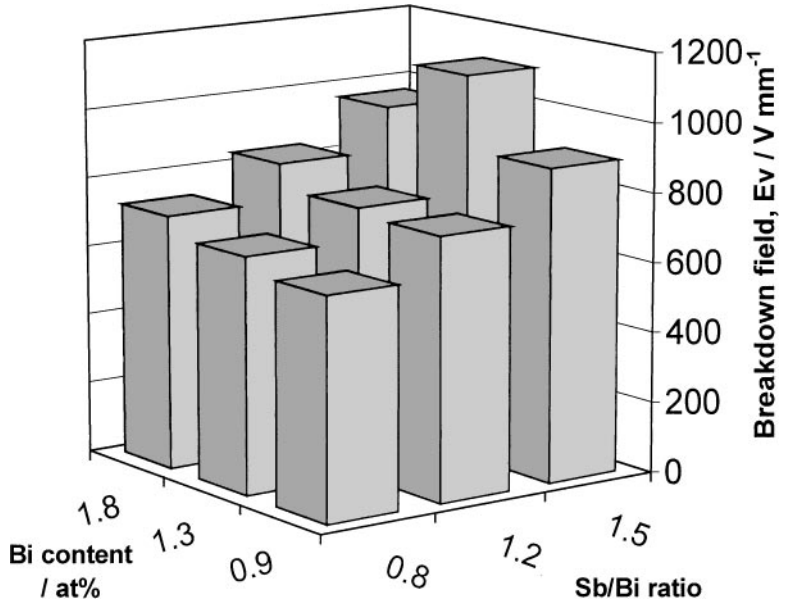

Fig. 3. Breakdown field E_V, for varistors of 0.9–1.8 at% Bi and 0.8–1.5 Sb/Bi ratio, sintered at 930°C.

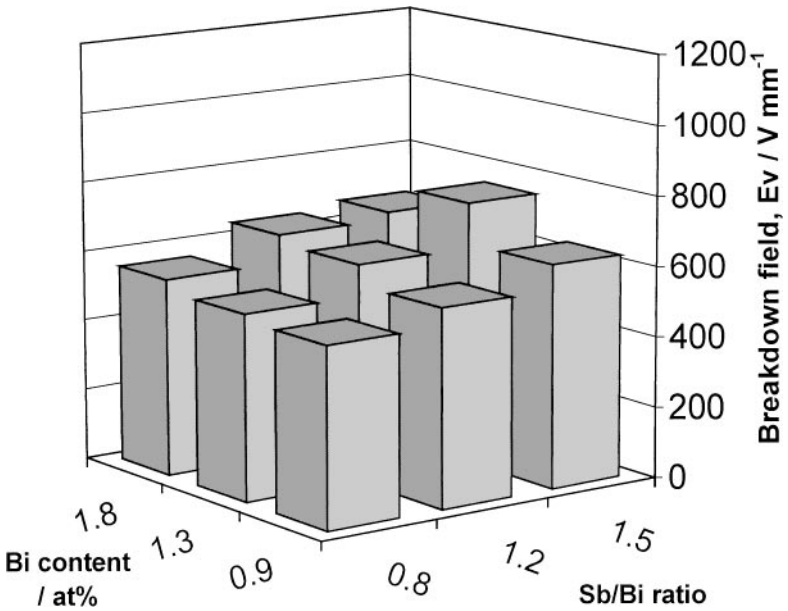

Fig. 4. Breakdown field E_V, for varistors of 0.9–1.8 at% Bi and 0.8–1.5 Sb/Bi ratio, sintered at 970°C.

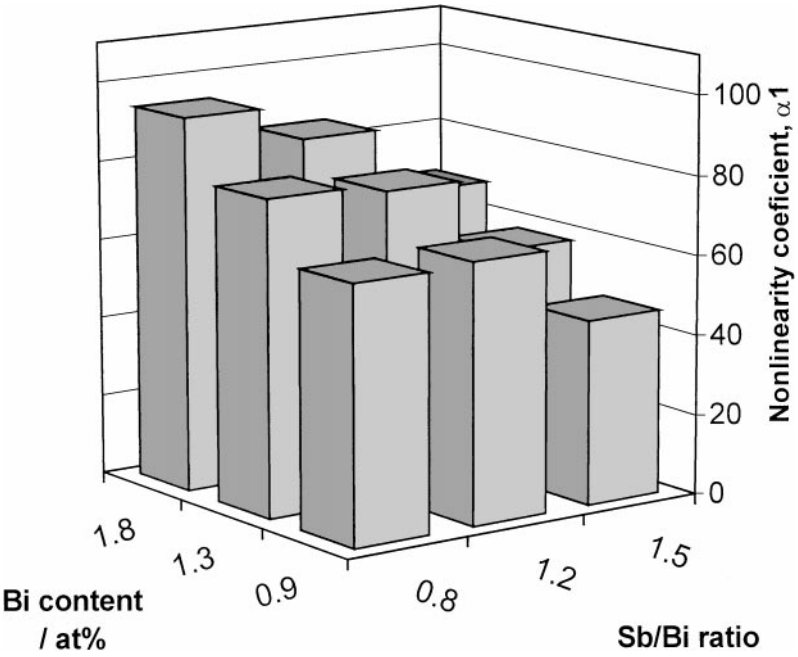

Fig. 5. Nonlinearity coefficients, $\alpha 1$, for varistors of 0.9–1.8 at% Bi and 0.8–1.5 Sb/Bi ratio, sintered at 930°C.

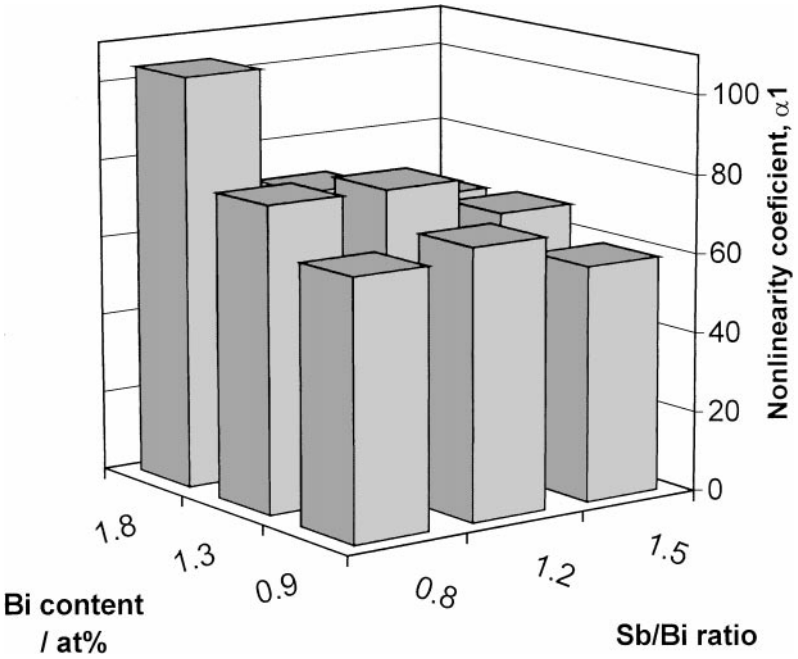

Fig. 6. Nonlinearity coefficients, $\alpha 1$, for varistors of 0.9–1.8 at% Bi and 0.8–1.5 Sb/Bi ratio, sintered at 970°C.

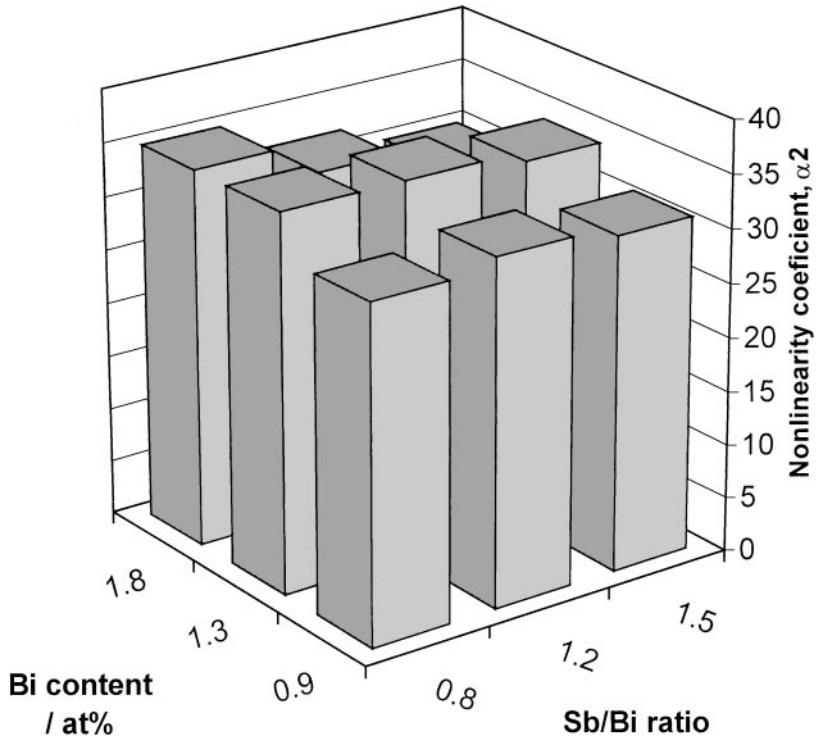

Fig. 7. Nonlinearity coefficient $\alpha 2$, for varistors of 0.9–1.8 at% Bi and 0.8–1.5 Sb/Bi ratio, sintered at 930°C.

extremely high value of 104 (sample 1b). From Fig. 5 it may be seen that, for the 930°C varistors, $\alpha 1$ increased with both increasing Bi content and decreasing Sb/Bi ratio. From Fig. 6 it may be noted that these trends are less easily discerned in the varistors sintered at 970°C, although for the highest Bi content and lowest Sb/Bi ratio the highest value of $\alpha 1$ was obtained. Overall, there was a slight increase in $\alpha 1$ for the higher temperature samples.

From Figs. 7 and 8 it may be seen that the calculated $\alpha 2$ values were distributed between 29 (sample 3b) and 36 (samples 5b). No clear trends were observed for the dependence of the $\alpha 2$ values on Bi content or Sb/Bi ratio, although the lowest values of $\alpha 2$ occurred at the highest Bi content and highest Sb/Bi ratios at both sintering temperatures. There was little difference in the $\alpha 2$ values between the samples sintered at 930°C and 970°C.

The influences of Bi content and the Sb/Bi ratio on W are shown in Figs. 9 and 10 (note that the Sb/Bi ratio changes along the axes in the opposite sense to that in Figs. 3–8). Clearly W increased with decreasing Sb/Bi ratio, but showed a less distinct trend with Bi content. The average values of W were higher for the 970°C samples (~700 J cm^{-3} compared with ~450 J cm^{-3}) although the range of values was large at each temperature.

Discussion

Equation (3) gives a relation between the microstructure of the varistor and the breakdown field E_V,

$$E_V = V_{gb} N_g \tag{3}$$

where V_{gb} is the voltage per intergranular boundary and N_g the number of grains per unit thickness. Previously, several researchers have shown that V_{gb} is almost independent of the composition of the varistor [24] and has a value between 3.0–3.6 V [9, 25]. Thus E_V may be used to approximate the number of grains between the electrodes. However, it should be noted however that if there was a wide distribution of grain sizes the

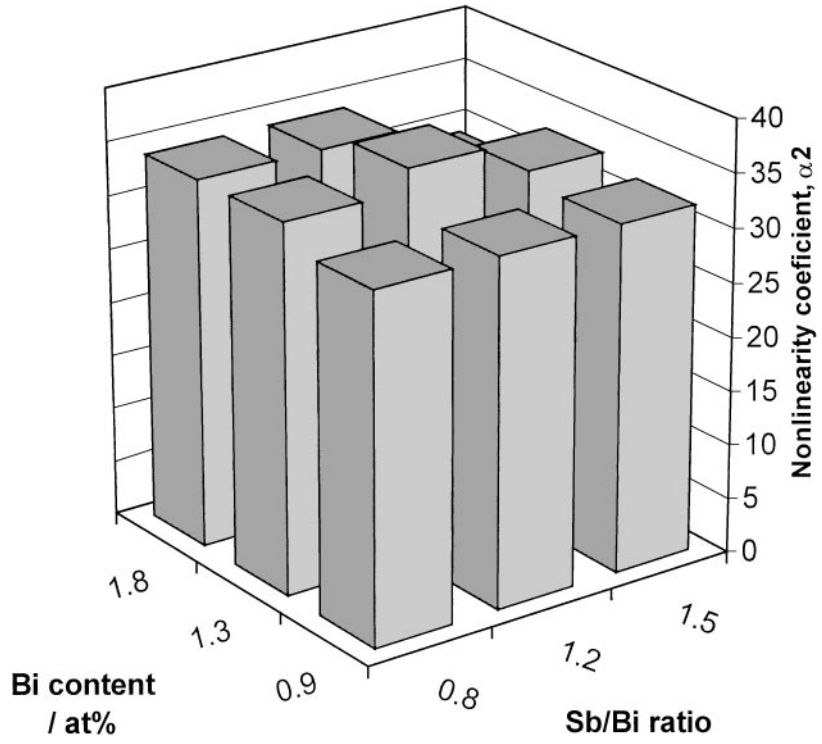

Fig. 8. Nonlinearity coefficient $\alpha 2$, for varistors of 0.9–1.8 at% Bi and 0.8–1.5 Sb/Bi ratio, sintered at 970°C.

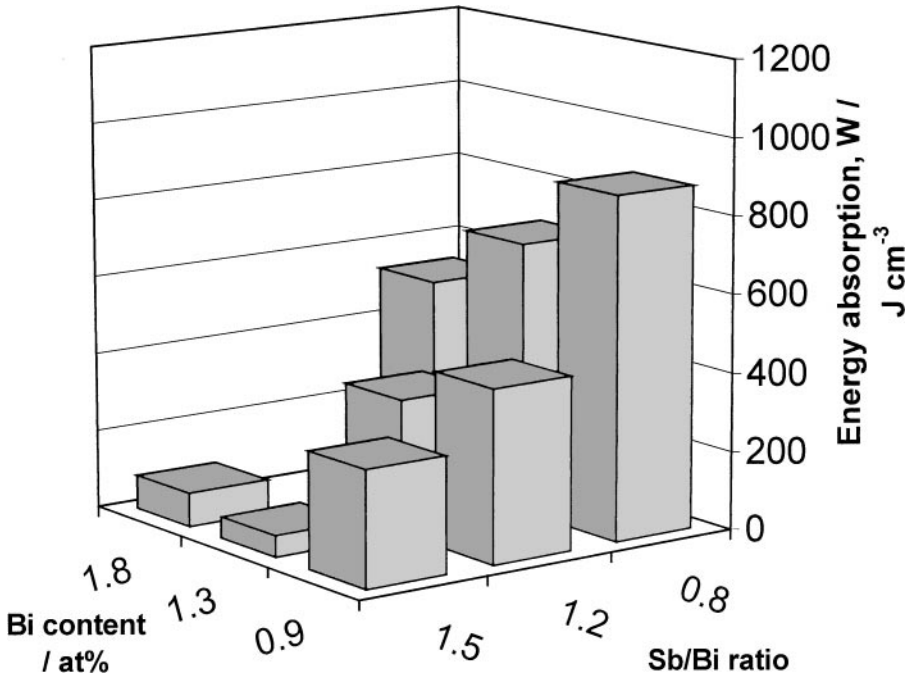

Fig. 9. Energy absorption capability W, for varistors of 0.9–1.8 at% Bi and 0.8–1.5 Sb/Bi ratio, sintered at 930°C.

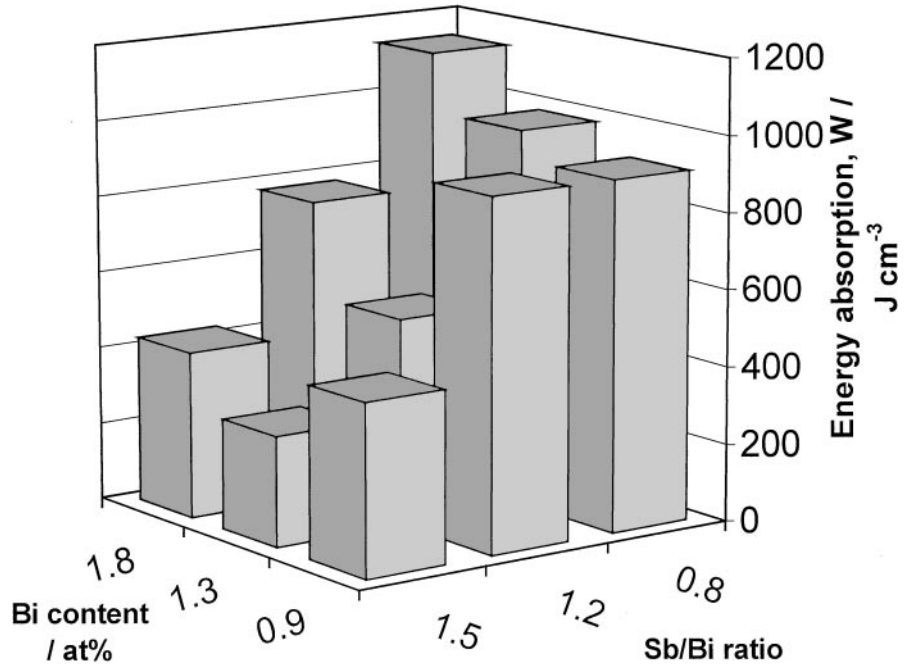

Fig. 10. Energy absorption capability W, for varistors of 0.9–1.8 at% Bi and 0.8–1.5 Sb/Bi ratio, sintered at 970°C.

conduction pathways would be dominated by the larger grains. Therefore, the characteristic grain size, determined from the breakdown field, is a reflection of the average size of the particles constituting the conduction pathways and will tend to be larger than the overall average grain size. Explicitly, if the characteristic grain size was small, many grains would be required to form the conduction pathways and E_V would be high. For the varistors examined in this study E_V was found to lie in the region 500–1000 V mm^{-1} (Figs. 3 and 4) indicating a characteristic grain size of 3–7 μm from Eq. (3). This is in good agreement with observations from scanning electron microscopy—a typical image (sample 9a) is shown in Fig. 1.

From the previous observations on the trends in E_V it may be concluded that the characteristic grain size was smaller at higher Bi concentrations, higher Sb/Bi ratio and at the lower sintering temperature. Also the range of characteristic grain sizes was greater at the lower sintering temperature.

The influence of the Sb/Bi ratio and the Bi content can be related to the inhibiting effect of the spinel phase $Zn_7Sb_2O_{12}$ on the grain growth of the ZnO grains [26, 27]. A controversial route to spinel has been proposed by Leite et al. [26] involving the formation of an intermediate trirutile phase Eq. (5), $ZnSb_2O_6$ at 700–800°C. Which in earlier work by Inada [28] was reported to be formed at 700–750°C.

$$ZnO + Sb_2O_5 \rightarrow ZnSb_2O_6 \tag{4}$$

Where the Sb_2O_5 is a liquid formed by oxidation of Sb_2O_3 with oxygen in the ambient atmosphere at 527°C. However, earlier work suggests that Sb_2O_5 decomposes at 525°C without forming a liquid phase [29]. Thus an alternative reaction may be envisaged:

$$ZnO + Sb_2O_3 + O_2 \rightarrow ZnSb_2O_6 \tag{5}$$

The $ZnSb_2O_6$ from Eqs. (4) or (5) may then undergo a solid-state reaction to form spinel (Eq. (6) > 800°C [26]) or pyrochlore (Eq. (7), 700 – 900°C depending on the additives [26]). It would be expected that no $ZnSb_2O_6$ remained above 900°C [28].

$$ZnSb_2O_6 + 6ZnO \rightarrow Zn_7Sb_2O_{12} \tag{6}$$

$$3ZnSb_2O_6 + 3Bi_2O_3 + ZnO \rightarrow 2Zn_2Bi_3Sb_3O_{14} \tag{7}$$

However the significance of the trirutile phase is not clear as the direct reaction, starting at 800°C, could

account for all of the spinel formation [16, 28] at temperatures below 900°C:

$$7ZnO + Sb_2O_3 + O_2 \rightarrow Zn_7Sb_2O_{12} \qquad (8)$$

However, at higher temperatures (>900°C [16, 28]) spinel is formed by decomposition of the pyrochlore phase Eq. (9), which was in turn formed during the earlier stages of sintering (>750°C [16]).

$$2Zn_2Sb_3Bi_3O_{14} + 17ZnO \Leftrightarrow 3Zn_7Sb_2O_{12} + 3Bi_2O_3(\text{liquid}) \qquad (9)$$

The last reactions Eqs. (8) and (9) are strongly influenced by additives which in general lower the reaction temperature, for example spinel formation has been observed at 600°C in a system with high additive concentrations [30].

The observation that with an increased Bi content and hence an increased Sb content, at a given Sb/Bi ratio, the characteristic grain size decreased can be explained by the increased amount of spinel that is formed via Eqs. (6) or (8).

To explain the influence of Sb/Bi ratio two different effects have to be taken into account. At Sb/Bi ratios <1 all Sb_2O_3 is consumed for the pyrochlore formation while a certain amount of liquid Bi_2O_3 remains present during the whole sintering process. This liquid phase enhances the grain growth. At Sb/Bi ratios >1 all Bi_2O_3 is consumed at relatively low temperatures by the formation of the pyrochlore. Similarly if any Sb_2O_5 were formed it would not have remained at much above 700°C as it would by consumed by the reaction in Eq. (6). Only at temperatures above 900°C at which Eq. (9) occurs a liquid phase is formed again. Antimony that is not incorporated into the pyrochlore can undergo reactions at temperatures above 800°C to form spinel (Eq. (6)). Therefore at Sb/Bi ratios >1 grain growth is hindered even in the early stages of sintering and higher breakdown fields E_V are obtained. At the higher sintering temperature it is clear that more liquid from Eq. (9) may be present for an extended period of time. Hence it is not unexpected that the grains appear larger after the higher temperature sintering.

Larger grains obviously imply fewer grain boundaries per unit thickness. The proportion of the total potential difference that appears across the grain boundaries, as opposed to the grain bulks, may be expected to be smaller for larger grained samples. Hence the nonlinearity coefficient $\alpha 1$ would be expected to be smaller when the grains are larger. However, the proportion of the potential difference across the grain bulks is likely to be vanishingly small at currents much below the upturn region of the *I/V* curve.

$\alpha 1$ is also influenced by the homogeneity and composition of the intergranular layers. It was observed that $\alpha 1$ was higher at high Bi, low Sb/Bi and only slightly affected by temperature. At high Bi concentrations or low Sb/Bi ratios more liquid phase (Bi_2O_3) would be present during the early stages of sintering. The liquid phase enhances the homogeneous distribution of barrier forming additives and hence homogeneous barrier formation [31]. In this study the influence of increased barrier homogeneity appears to exceed that of increased characteristic grain size in determining $\alpha 1$. Current passes through a varistor via a number of discrete conduction channels [31]. $\alpha 2$ would be expected to have a higher value if there were a large number of conduction pathways through the sample (narrow distribution of particle sizes or absence of abnormally large grains) and if the intergranular regions were homogeneous. The low values of $\alpha 2$ at high Bi and Sb concentrations (Figs. 7 and 8) may be indicative of a large amount of inactive (spinel and pyrochlore) material in the intergranular regions leading to fewer, more tortuous conduction pathways.

A high W value would be expected for varistors in which the energy of the test pulse is uniformly dissipated by the entire volume of the pellet. Varistors in which energy is dissipated by a fraction of the pellet volume would undergo localised heating in a few regions. Such non-ideal varistors would be liable to fail at relatively low overall energies, by cracking or puncture [2]. The observed values of W (54–1137 J cm^{-3}) indicate that at least some of the pellets heated in a distinctly non-uniform fashion in agreement with simulations [32, 33] and experimental electroluminescence observations [31]. From the low $\alpha 2$ values it was anticipated that the quality and quantity of conduction pathways in samples with the highest Bi and Sb concentrations might be low. In support of this hypothesis the W values are also low in this region. Additionally the W values may also be expected to be a sensitive measure of the pellet homogeneity (and hence to be dependent on similar factors to $\alpha 1$). W like $\alpha 1$ was observed to increase with decreasing Sb/Bi ratio. However, there was also a strong correlation between the characteristic grain size (from Eq. (3) with V_{gb} taken as 3.3 V) and W, Fig. 11. It appeared

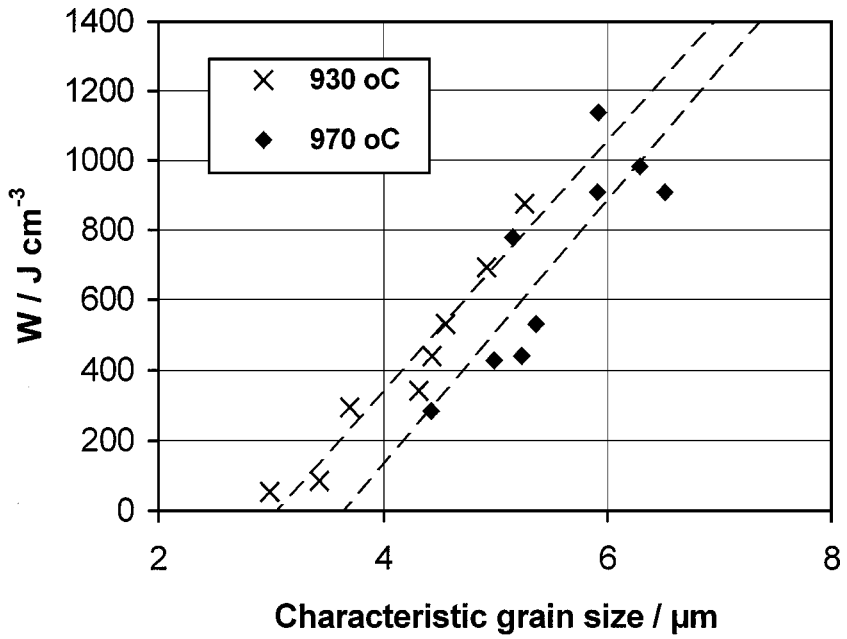

Fig. 11. Energy absorption capability W, arranged against the characteristic grain size determined from E_V through Eq. (3). The linear regressions are provided as a guide to the eye only.

that the energy absorption ability of varistors was increased by larger characteristic grain sizes. It may be noted that smaller grains sinter more readily than larger grains. If the grains had fused together as a consequence of localised heating induced by the test pulse the characteristic grain size would have increased, reducing the value of E_V. The temperatures, and hence energies, required to sinter the grains would be significantly lower for smaller-grained pellets. As a change in E_V was taken as one indicator of sample failure, small-grained pellets would have been more likely to fail by this mode than large-grained samples.

Also from Fig. 11 it may be noted that for pellets with similar characteristic grain sizes the pellets sintered at the higher temperatures had a lower energy absorption ability. At first, especially given the higher densities of the 970°C samples, this result appeared counter-intuitive. However, for a given characteristic grain size the pellets sintered at 970°C had higher amounts of additives (Sb and Bi) and therefore the amount of pyrochlore and spinel would be expected to be greater. It may be assumed that the pyrochlore and spinel phases restricted the number (or width) of conducting channels and hence reduced the energy which could be tolerated by the samples. Therefore, in summary,W was dependent on grain size, homogeneity and total amount of spinel and pyrochlore phases.

Conclusions

The studied compositions with a Bi-content of 0.9 to 1.8 at% and an Sb/Bi ratio of 0.8 to 1.5 led to dense varistor ceramics at sintering temperatures of 970°C and 930°C. At the higher temperature the growth of ZnO grains increased and hence the number of grains per unit thickness decreased, leading to lower values of E_V. However, by increasing the Sb/Bi ratio or the Bi concentration the grain growth could be inhibited, presumably by the formation of a spinel phase ($Zn_7Sb_2O_{12}$). The more and the earlier the spinel phase was formed during the sintering process the higher E_V, however too much spinel (or pyrochlore) formation may have caused a reduction in the number of conduction pathways, leading to low $\alpha 2$ and W values.

The nonlinearity coefficient $\alpha 1$ could be varied from 46 to 104 by increasing the Bi concentration and temperature. The explanation proposed here was that a larger amount of liquid Bi_2O_3 resulted in a more homogeneous distribution of extragranular, minor

components, which led to more homogeneous barrier formation and higher $\alpha 1$ values.

The energy absorption ability of the varistors increased with increasing characteristic grain size and decreasing Sb/Bi ratio. Therefore it may be speculated that, in this system at least, there will have to be a compromise between the desirable properties of high E_V and high W.

Acknowledgments

We thank Siemens-Matsushita (now EPCOS OHG) for providing materials. Discussion with J. Schoonman is gratefully acknowledged.

References

1. M. Matsuoka, *Jpn. J. Appl. Phys.*, **10**, 736 (1971).
2. M. Bartkowiak, M.G. Comber, and G.D. Mahan, *J. Appl. Phys.*, **79**, 8629 (1996).
3. S. Ezhilvalavan and T.R.N. Kutty, *J. Mater. Sci.*, **7**, 137 (1996).
4. J. Fan and F.R. Sale, in *Electroceramics: Production, Properties and Microstructures*, edited by W.E. Lee and A. Bell (Ashgate Publishing Company, London, 1994), p. 151.
5. J. Fan and R. Freer, *J. Mater. Sci.*, **32**, 415 (1997).
6. T.K. Gupta, *J. Mater. Res.*, **7**, 3280 (1992).
7. M.C.S. Nobrega and W.A. Mannheimer, *J. Am. Ceram. Soc.*, **79**, 1504 (1996).
8. G.M. Safronov, V.N. Batog, T.V. Stepanyuk, and P. Fedorov, *Russ. J. Inorg. Chem.*, **16**, 460 (1971).
9. E. Olsson and G.L. Dunlop, *J. Appl. Phys.*, **66**, 3666 (1989).
10. E. Olsson, L.K. Falk, and G.L. Dunlop, *J. Mater. Sci.*, **20**, 4091 (1985).
11. H. Wang and Y.-M. Chiang, *J. Am. Ceram. Soc.*, **81**, 89 (1998).
12. E. Olsson, G. Dunlop, and R. Österlund, *J. Am. Ceram. Soc.*, **76**, 65 (1993).
13. D. Dey and R.C. Bradt, *J. Am. Ceram. Soc.*, **75**, 2529 (1992).
14. J. Kim, T. Kimura, and T. Yamaguchi, *J. Am. Ceram. Soc.*, **72**, 1541 (1989).
15. T. Asokan, G.N.K. Iyengar, and G.R. Nagabhushana, *J. Mater. Sci.*, **22**, 2229 (1987).
16. M. Inada and M. Matsuoka, *Jpn. J. Appl. Phys.*, **19**, 409 (1980).
17. J.L. Huang and K.B. Li, *J. Mater. Res.*, **9**, 1526 (1994).
18. O. Alvarez-Fregoso, *Rev. Mex. Fisica*, **40**, 771 (1994).
19. M. Ito, M. Tanahashi, M. Uehara, and A. Iga, *Jpn. J. Appl. Phys.*, **36**, 1460 (1997).
20. A. Mergen and W.E. Lee, *J. Europ. Ceram. Soc.*, **17**, 1049 (1997).
21. A. Lorenz, J. Ott, M. Harrer, E.A. Preissner, A.H. Whitehead, and M. Schreiber, *J. Electroceram. Soc.*, **6**, 43 (2001).
22. T.K. Gupta, *J. Am. Ceram. Soc.*, **73**, 1817 (1990).
23. L.M. Levinson and H.R. Philipp, *Ceram. Bull.*, **65**, 639 (1986).
24. W.G. Morris, *J. Vac. Sci. Technol.*, **13**, 926 (1976).
25. R. Einzinger, *Appl. Surf. Sci.*, **1**, 329 (1978).
26. E.R. Leite, M.A.L. Nobre, E. Longo, and J.A. Varela, *J. Mater. Sci.*, **31**, 5391 (1996).
27. V. Kraševec, M. Trontelj, and L. Golič, *J. Am. Ceram. Soc.*, **74**, 760 (1991).
28. M. Inada, *Jap. J. Appl. Phys.*, **17**, 1 (1978).
29. H. Honning and E.J. Kohlmeyer, *Erzbergerbau Metallüettenw.*, **10**, 12 (1957).
30. Y.S. Lee and T.Y. Tseng, *J. Mater. Sci.: Materials in Electronics*, **8**, 115 (1997).
31. F. Greuter, T. Christen, and J. Glatz-Reichenbach, *Mat. Res. Soc. Symp. Proc.*, **500**, 235 (1998).
32. A. Vojta and D.R. Clarke, *J. Appl. Phys.*, **81**, 985 (1997).
33. M. Bartkowiak and G.D. Mahan, *Phys. Rev. B*, **51**, 10825 (1995).